Island Arc

Island Arc (2012) **21,** 66–78

Research Article

Effects of tides and weather on sedimentation of iron-oxyhydroxides in a shallow-marine hydrothermal environment at Nagahama Bay, Satsuma Iwo-Jima Island, Kagoshima, southwest Japan

SHOICHI KIYOKAWA,[1,2]* TOMOMI NINOMIYA,[1,†] TOMOAKI NAGATA,[1] KAZUMASA OGURI,[3] TAKASHI ITO,[4] MINORU IKEHARA[5] AND KOSEI E. YAMAGUCHI[6,7]

[1]*Department of Earth and Planetary Sciences, Kyushu University, 6-10-1 Hakozaki Higashiku, Fukuoka 813-8581, Japan (email: kiyokawa@geo.kyushu-u.ac.jp)*, [2]*Department of Geology, University of Johannesburg, Auckland Park Kingsway campus, Auckland Park 2006, Johannesburg, South Africa*, [3]*Institutes of Biogeosciences, Japan Agency for Marine-Earth Science and Technology, Yokosuka 237-0061, Japan*; [4]*Faculty of Education, Ibaraki University, Mito 310-8512, Japan*, [5]*Center for Advanced Marine Core Research, Kochi University, Nankoku, 783-8502 Japan*, [6]*Department of Chemistry, Toho University, Funabashi, 274-8510 Japan*; *and* [7]*NASA Astrobiology Institute*

Abstract Nagahama Bay of Satsuma Iwo-Jima Island, southwest Japan, is an excellent place for studying sedimentation of iron-oxyhydroxides by shallow-marine low-temperature hydrothermal activity. Its fishing port has a narrow entrance that limits exchange of seawater between the bay and open ocean, allowing the accumulation of fine-grained precipitates of iron-bearing materials (Fe-oxyhydroxides) on the seafloor. The fishing port is usually filled with orange- to brown-colored Fe-rich water, and deposits >1.5 m thick Fe-rich sediments. To elucidate the movement and depositional processes of the Fe-rich precipitates in the bay, we conducted continuous profiling of turbidity throughout the tidal cycle and monitoring of surface water. The results showed that clear seawater entered the bay during the rising tide, and turbid colored water flowed into the ocean during the ebb tide. Neap tide was found to be an optimal condition for sedimentation of Fe-oxyhydroxides due to weak tidal currents. Storms and heavy rains were also found to have influenced precipitation of Fe-oxyhydroxides. Storm waves disturbed the bottom sediments, resulting in increased turbidity and rapid re-deposition of Fe-oxyhydroxides with an upward-fining sequence. Heavy rain carried Fe-oxyhydroxides originally accumulated in nearby beach sands to the bay. Our findings provide information on optimal conditions for the accumulation of Fe-rich sediments in shallow-marine hydrothermal settings.

Key words: Fe-oxyhydroxides, hot spring, rain, shallow-marine, storm, tide.

INTRODUCTION

Iron-rich sedimentary sequences provide a key to understanding the paleoenvironmental roles of oxygen and hydrothermal activity in the ocean (e.g. Holland 1984; Condie 1997). Previous studies of iron deposits have classified iron sedimentation in different settings such as: (i) bog iron ores (Stanton 1972); (ii) ironstone (mainly oolite; Young & Taylor 1989); and (iii) banded iron formations (BIFs; e.g. Robb 2005).

Bog iron ores are formed in lacustrine and swamp environments associated with glaciated terrain and tundra (Stanton 1972). In this setting, the Fe^{2+}-rich pore water from anoxic sediments precipitates the ores by mixing with oxidized surface water, as having been observed in modern

*Correspondence.

Current Address: †Geology & Geophysics Support, Schlumberger Information Solutions, Tokyo 104-0028, Japan.

Received 1 September 2011; accepted for publication 14 January 2012.

doi:10.1111/j.1440-1738.2012.00808.x

environments where swamps discharge into downstream drainage areas. Ironstone deposits with oolitic appearance usually formed in shallow-marine and deltaic environments by wave agitation. These deposits are mainly Phanerozoic and often associated with organic-rich black shales that mark stages of major marine transgression and flooding of the continental margin (Young & Taylor 1989). The source of the iron is considered to be weathering and oxidation of lateritic soils (Young & Taylor 1989). Ironstones can also be associated with submarine volcanic activity in platform settings (Siehl & Thein 1989). BIFs are bedded chemical sediments that consist of alternating Fe-rich and Si-rich layers (Klein & Beukes 1993). They are generally grouped as Algoma, Lake-Superior, or Rapitan types. The source of Fe is thought to have been hydrothermal activity in subaqueous environments. Models of the BIF formation include the upwelling model (Klein & Beukes 1993), Red Sea model (Ohmoto *et al.* 2006), microbial mediation model (Konhauser & Ferris 1996; Takashima *et al.* 2011), and alkaline–ocean model (Shibuya *et al.* 2010).

Bog iron, ironstone, and BIFs are lithologically distinct. Bog iron consists of thin beds containing local terrestrial detritus, ironstone forms mainly massive layers containing oolites, and BIFs are distinguished by well-defined laminations. The depositional mechanisms for these iron deposits remain uncertain because it is difficult to observe the behavior of oxidized ferric matter in the ocean. Most depositional models assume that oxidation of Fe^{2+} occurs when dissolved Fe^{2+} is oxidized to be essentially insoluble Fe^{3+} with either increasing Eh or pH. However, the subsequent behaviors of Fe^{3+}-bearing colloids are poorly understood. In marine environments, Fe^{3+}-bearing colloids may be intermediate materials in the formation of thick Fe-rich layers. The fate of Fe^{3+} is thus important in understanding the entire process for the formation of Fe-rich layers in sedimentary sequences.

Hydrothermal vents are often surrounded by colored seawater, but no thick accumulation of iron hydrate sediments has been reported in these particular areas (e.g. Tarasov *et al.* 1999, 2005). To better understand sedimentary mechanisms of Fe-rich layers under shallow-marine hydrothermal environments, we carried out an observational study in Nagahama Bay of Satsuma Iwo-Jima Island, southwest Japan. The island, approximately 50 km south of Kyushu Island, is characterized by shallow-water hydrothermal activity where orange-brown and brown-white discharges can be found along the shoreline. Such coloring occurs due to precipitation of Fe- and Al-bearing minerals as a result of the neutralization and oxidation of acidic hydrothermal fluids that contain high concentrations of Fe and Al (Kamada 1964; Nogami *et al.* 1993; Shinohara *et al.* 1993; Hedenquist *et al.* 1994). The iron-rich hydrothermal discharge of clear hot spring water around the island is quickly colored after mixing with seawater, which induces ferric iron precipitation. The colored water diffuses into a rocky and pebbly coastline of the island, which is subject to strong wave action and ocean currents. These hydrological factors make it difficult to study depositional mechanisms for iron hydrate (or oxides) along the coastline.

A fishing port constructed in the innermost portion of Nagahama Bay is protected from wave action by artificial breakwaters. This setting is expected to allow the deposition of Fe-oxyhydroxides. Preliminary sediment sampling in the fishing port recovered Fe-oxyhydroxide-rich sediments of more than 1 m-thick. The protected nature of the fishing port would provide a unique opportunity to better understand the formation of Fe-rich sediments.

The source and movement of Fe-bearing particles are difficult to observe in detail due to the opacity of the water at the study sites, but can be traced by measuring water turbidity. We performed long-term observations for the movement of the orange-brown water from fixed locations, to examine the influence of the tidal currents in the bay. Our findings provide information on the optimal conditions for the accumulation of iron-rich sediments in marine hydrothermal settings.

GEOLOGICAL SETTING OF SATSUMA IWO-JIMA ISLAND

Satsuma Iwo-Jima Island (Fig. 1) is in the northwestern rim of the mostly submerged Kikai Caldera (Matsumoto 1943), where a huge eruption at 7.3 kya produced the Akahoya tephra, an extensive and well-studied material in Japan (e.g. Machida & Arai 1978; Maeno & Taniguchi 2007, 2009). The island is an active volcano 5.5 km long from east to west and 4 km wide from north to south. The north and west sides of the island are thick basaltic cliffs of the remaining caldera structure (dashed line in Fig. 1). Two post-caldera volcanoes exist within the main caldera: the steep rhyolitic Iwo-dake, and the basaltic cinder cone

Inamura-dake (Ono *et al*. 1982). Iwo-dake was formed from an eruption approximately 610–500 years ago (Kawanabe & Saito 2002) and is still active today, as evidenced by fumarolic gas of 902°C measured at the summit area in 1994 (Shinohara *et al*. 2002).

The low-temperature hydrothermal fluids around Satsuma Iwo-Jima Island have a mild acidity (approx. pH 5) due to the presence of carbonic acid. It also contains high concentrations of Al and Fe (up to 1250 and 649 mg/L, respectively; Kamada 1964). Along the coastline of the island, the low-temperature hydrothermal fluids are neutralized by the surrounding seawater, resulting in the precipitation of Fe- and Al-bearing minerals. The coloring of seawater into ivory or orange-brown are due to $Al(OH)_3$ and $Fe(OH)_3$, respectively, and occurs adjacent to beaches at Iwo-dake volcano. Iron-rich microbial precipitates have been reported from the coastline around the Akaiwa area and in Nagahama Bay (Shikaura & Tazaki 2001).

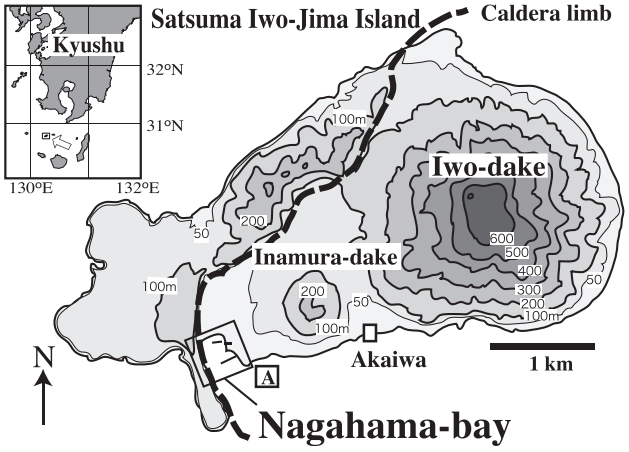

Fig. 1 Topographic map of Satsuma Iwo-Jima Island. The square labeled 'A' indicates the area shown in Figure 2b.

SAMPLING SITES IN NAGAHAMA BAY

The orange-brown-colored hydrothermal fluids are most prominent in Nagahama Bay in Satsuma Iwo-Jima Island (Fig. 1). Before the construction of several breakwaters, the bay was a sandy beach steeply declining to the open ocean, which allowed quick outflow of orange-brown water. As shown in Figure 2a, the port's narrow entrance is protected by two breakwaters at the southern end. The port has a 200 m-long concrete ferry berth along its east side and a T-shaped quay for small fishing boats. Along the coastline of the island, the port is the only place that retains the large volume of orange-brown water. The port is divided into east and west sides (E site and W site, respectively) by the T-shaped quay (Fig. 2b). Sediment dredging was performed in 1983, 1984, 1986, 1989, and 1991 at the E site and in 1997 at the W site (Ninomiya & Kiyokawa 2009). After construction of the

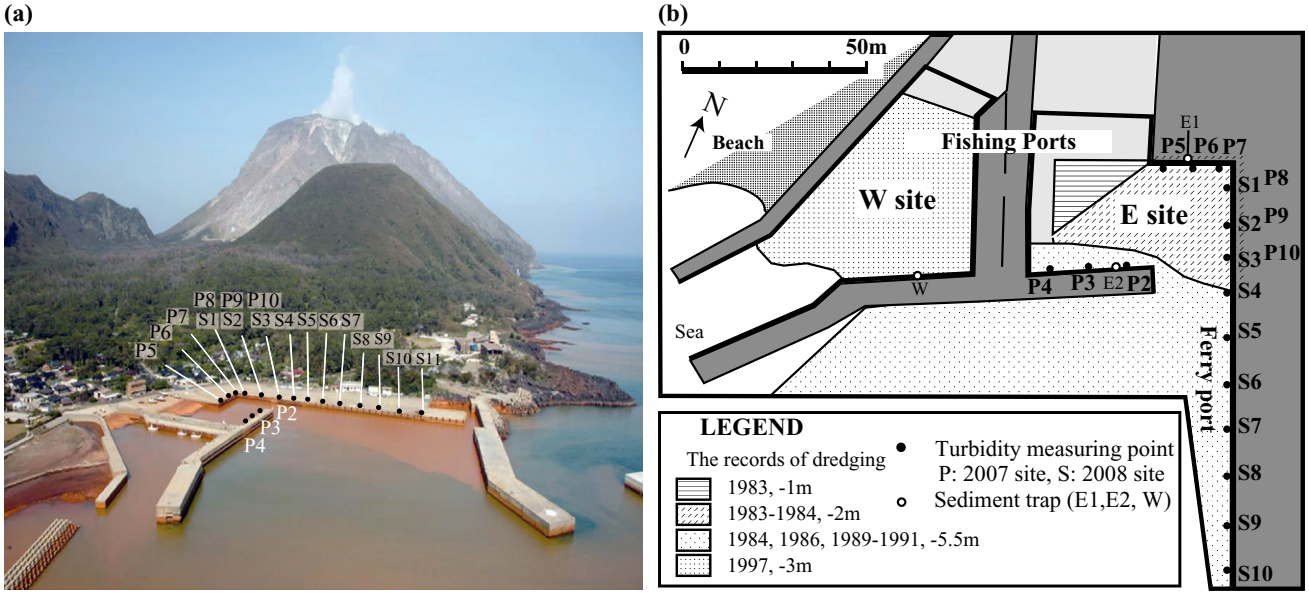

Fig. 2 (a) Overview of Nagahama Bay. (b) Dredging record at the fishing port (E and W sites) in Nagahama Bay (Kagoshima Prefecture 2008). In (a) and (b), sites of turbidity measurements in 2007 are labeled P2–P10; those in 2008 are labeled S1–S10. E1, E2, and W1 denote sites for sediment trap experiments.

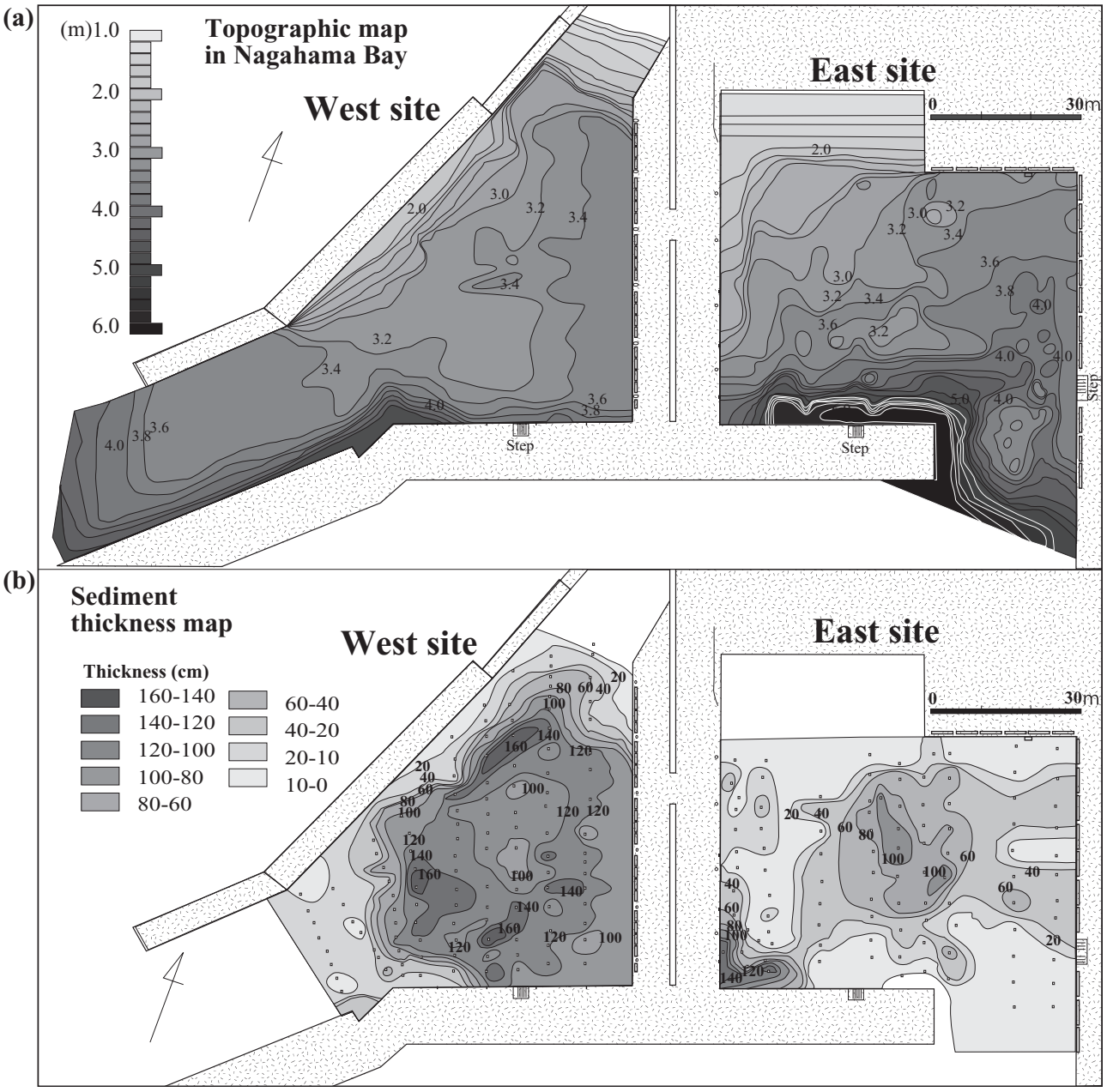

Fig. 3 (a) Bathymetric map of Nagahama Bay (data after Ninomiya & Kiyokawa 2009). (b) Map of sediment thickness in Nagahama Bay in 2008. Dots indicate measurement points.

wharves, the bay became calmer and favorable for sediment accumulation. The persistent presence of orange-brown water in this area indicates that hydrothermal activity remains active on the basin floor of the E and W sites.

Bottom sediments of more than 1 m in thickness were dredged from the W site during 15–25 June 2009. A 10 m-wide area along the eastern part of the W site was not dredged (Fig. 2b). We collected data on the sediment thickness and water depth in 2008 by using a 6 m-long bamboo stick that was pushed through the sediment until it touched hard rock basement or sandy substrate. Depth and thickness data were cross-checked with line profiles using an echo-sounder (PS-50C; Honda Electronics Co., Toyohashi, Japan) on a small rubber raft (FMI-332; Achilles Co., Tokyo, Japan) (see Fig. 3). The bathymetric data shown in Figure 3a were based on water depth during typical low tide, which was 50 cm deeper than the depth in the lowest tide level during spring tide. The E and W sites have different bathymetric profiles. The

W site has a relatively flat seafloor and is shallower in the center. The E site gradually slopes toward the open sea and is more than 6 m deep along the T-shape quay (Fig. 3a). Several small mounds (<1 m in height) occur in the central area of the E site. A cluster of mounds occurs in a 5 m × 6 m area near the eastern entrance of the fishing port.

The thickness of unconsolidated surface sediment at the W site is greater than 1 m in the middle of the basin, with a maximum of 1.5 m in the central and eastern parts of the site. The E site sediments were thinner and much coarser than those of the W site, and consisted of 20–80 cm-thick Fe-rich mud and volcanic sand. The southwestern corner of the E site was covered by a 1.0–1.3 m-thick layer of mud (Fig. 3b). For port maintenance at E site, >1 m-thick bottom sediments were dredged from the W site during 15–25 June 2009; however, a 10 m-wide area along the eastern part of the W site was kept from dredging for preserving samples for our scientific research (see Fig. 2b).

We estimated the sedimentation rate in Nagahama Bay by using a simple sediment trap device consisting of a pair of 2 L bottles. The trap was positioned 1 m above the seafloor at locations E1 and W for 203 days (6 September 2006 to 29 March 2007; see Fig. 2). The estimated sedimentation rates at these points were 3.6 g/cm^3/month at E1 and 5.4 g/cm^3/month at W, consistent with the measurements of overall sediment thickness at these sites (Fig. 3b) and the construction of the longer breakwaters at the W site.

In addition to bathymetric measurements, we obtained underwater images using an 'Oguri-view' system (underwater long-term recording camera system attached with a flashbulb and a timer) (e.g. Oguri *et al.* 2006) The images showed muddy, red to brown bottom sediments with ripple marks at the W site during high tide. The sediments contained small pockmarks with widths of <5 cm and depths of 2–3 cm.

TURBIDITY MEASUREMENTS

To understand the daily and monthly hydrological changes in Nagahama Bay, we monitored the turbidity associated with mixing of the orange-brown hydrothermal fluids and seawater (Figs 4,5). Using a multiple sensor (WX-22; Horiba), depth profiles of the turbidity and pH were measured 5 times at 50 cm intervals from the surface to the bottom. The deepest point was 8 m at high tide, and the shallowest point was 2 m at low tide. Data were collected during relatively calm periods from 23 September to 7 October 2007 (Fig. 4) and from 3 to 12 August 2008 (Fig. 5). Timings of measurement are shown in tidal timetables provided by the Japan Meteorological Agency (Figs 4a,5a), and were usually carried out four times a day (at high, ebb, low, and incoming tides).

To monitor changes in turbidity, specific measuring points were selected along the port quays. Two sections were set along the T-shaped quay (P2–P4) and the northeastern quay (P5–P10; Fig. 2b) for the measurements in 2007. These are referred as the East fishing port section. For the measurements in 2008, another section was set along the ferry port quay (S1–S10) and is referred as the Ferry port section (Fig. 2b). The sites P8, P9, and P10 correspond to S1, S2, and S3, respectively. A nephelometric turbidity unit (NTU) was used to quantify the turbidity. One NTU corresponds to the turbidity of water containing 1 mg/L of finely dissolved silica. Clear water has a value of 0 NTU.

TIME-SERIES CROSS-SECTION IMAGES OF TURBIDITY

Cross-sectional images of the turbidity data were drawn using Ocean Data View (ODV) software (http://odv.awi.de). Wave height data (Figs 4a,5a) were corrected with reference to ladder steps on the side of the quay at the fishing port.

The turbidity data of the East fishing port and the ferry port clearly show tidal effects on the daily and longer term changes (Figs 4,5). The turbidity change followed a daily cycle of tidal currents. At high tide, both data sets show that the clear seawater (<10 NTU) flowed into the bay along the sea bottom. Turbidity increased during the ebb tide, as clearly seen in the fishing port section (from 20 to 80 NTU; Fig. 4b). High turbidity persisted until seawater came in during the rising tide.

The turbidity data also responded to longer term changes in the amplitude of the daily tide, as seen in the data from 23 September 2007 to 4 October 2007 (Fig. 4) and from 3 to 12 August 2008 (Fig. 5). Both datasets show changes in response to the transition from less turbid water during the spring tide to more turbid water during the neap tide. High turbidity during the neap tide from 4 to 7 September 2007 could have been affected by a typhoon; however, the turbidity change in the 2008 data reflects a long-term tidal situation during fair weather.

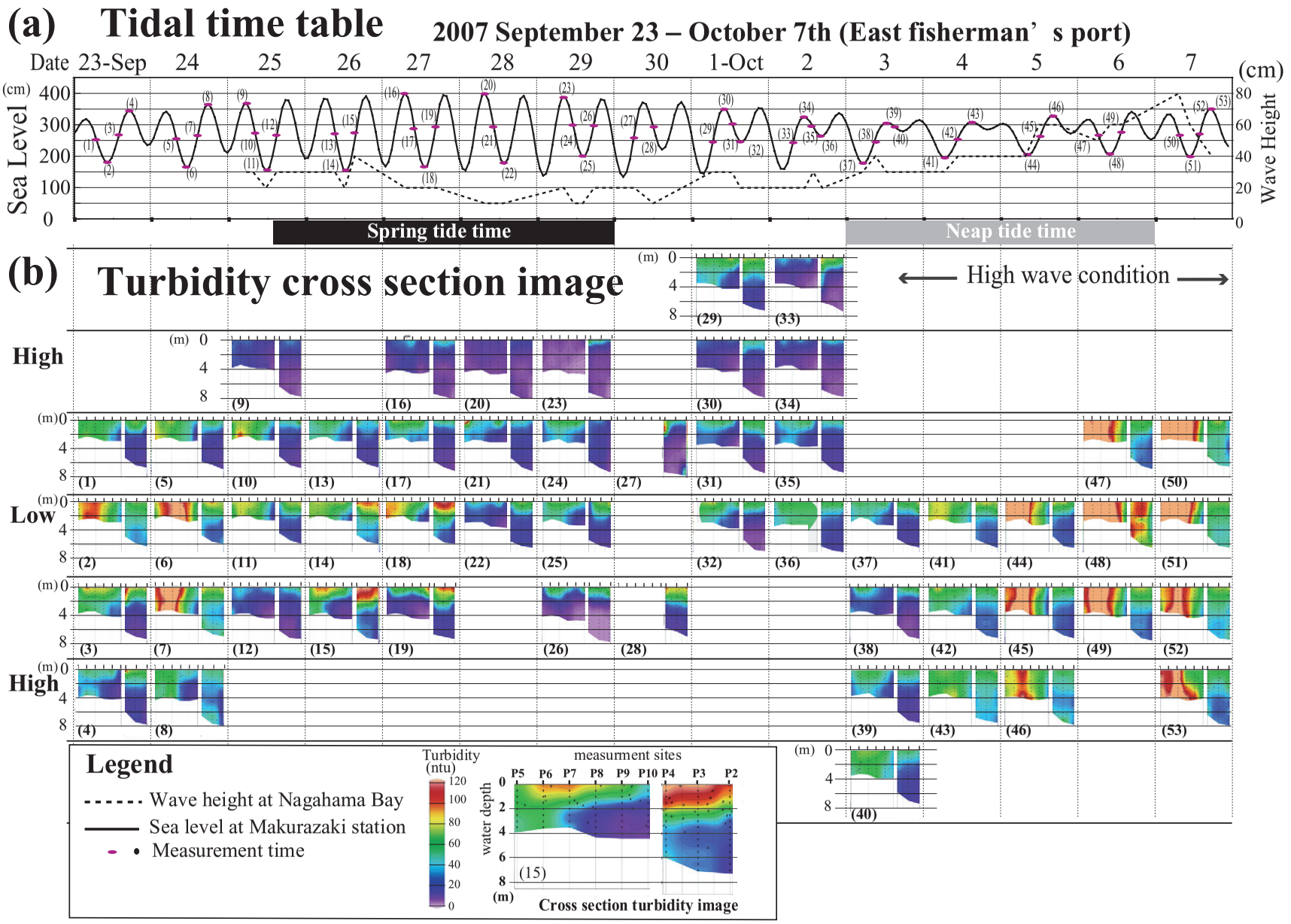

Fig. 4 (a) Tide tables for Nagahama Bay from 27 September 2007 to 7 October 2007 (data from Ninomiya & Kiyokawa 2009). Solid line indicates the approximate water level at Satsuma Iwo-Jima Island, based on tide data from the proximal tidal level station of the Japan Meteorological Agency at Makurazaki port, which is 50 km from Iwo-Jima Island. Red dots indicate times when the water turbidity was measured. Numbers (1)–(53) correspond to the cross-sectional images. (b) Turbidity cross-sectional images within the east fishing port (P2–P4) and along the ferry port (P5–P10). Measurement sites for the cross-sectional images along P2–P4 and P5–P10 are shown in Figure 2. The color chart on the right side of each image shows the minimum value of 0 NTU (purple) and the maximum value of 120 NTU (orange). Data in (a) from Ninomiya and Kiyokawa (2009).

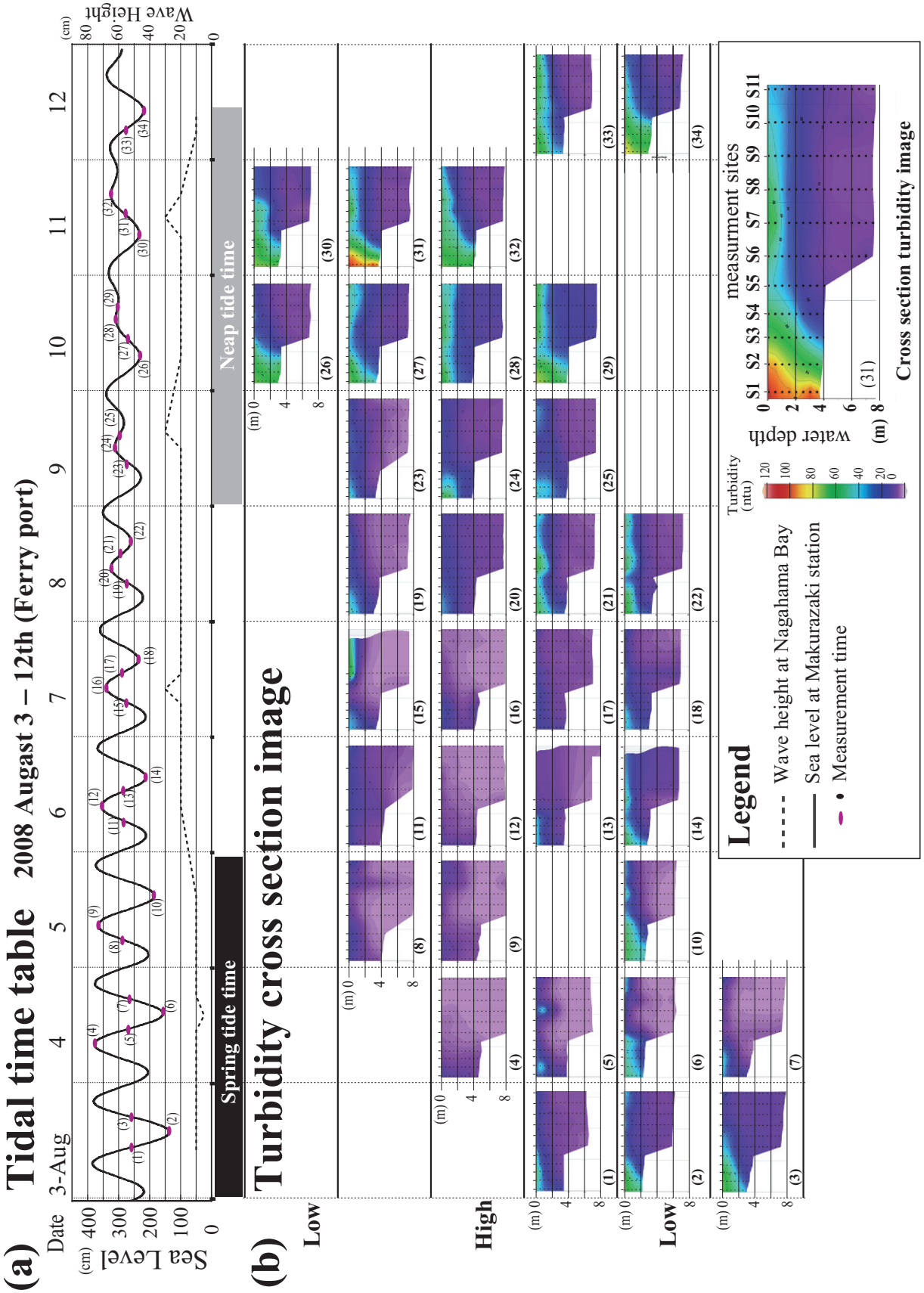

Fig. 5 (a) Tide tables for 3–12 August 2008. Solid line indicates the approximate water level at Satsuma Iwo-Jima Island, based on tide data from the proximal tidal level station of the Japan Meteorological Agency at Makurazaki port, which is 50 km from Iwo-Jima Island. Red dots indicate times when measurements were made. Numbers (1)–(34) correspond to the cross-sectional images. (b) Cross-sectional images of turbidity at the ferry port. Measurement sites for the cross-sectional images along S1–S11 are shown in Figure 2.

Long-term turbidity change likely resulted from the intensity of the seawater influx, which responded to the amplitude of tidal change. During the spring tide, the intense influx of clear seawater (<10 NTU) to the fishing port from the outer ocean resulted in a decrease in the turbidity. During the neap tide, seawater influx was lower and the turbidity was higher (Fig. 5).

Observations in August 2008 show that the turbidity in deeper parts of the water column is always lower than in shallower parts. When a typhoon occurred during 4–7 October 2007, strong waves at the E site resulted in enhanced turbidity of the water. During the storm, turbidity of >120 NTU was recorded in the shallow portion of the East fishing port. This was likely due to suspension of unconsolidated sediments because some of the profiles of storm periods show higher turbidity in deeper parts (Fig. 4).

Ninomiya and Kiyokawa (2009) reported a range in pH (about 7.2–8) in the bay. The pH and turbidity showed a negative correlation during fair weather. Lower pH values (pH 7.2) were associated with higher turbidity (60 NTU), whereas higher pH values (pH 8) were associated with turbidity of <10 NTU. These results are consistent with our interpretation that turbidity is related to the influx of seawater and its interactions with acidic water from local hot spring activity within the bay. During the storm event, the correlation between pH and turbidity was further strengthened (Ninomiya & Kiyokawa 2009).

COLOR CHANGES OF THE OCEAN SURFACE

Influences of tide and storm on the turbidity were confirmed by images obtained using the automatic camera recording system, which clearly shows the expansion and contraction of orange-brown waters within Nagahama Bay (Fig. 6). Surface waters covering the study area were monitored by the system, over short-term (30 s) and long-term (30 min) intervals, installed at a hilltop location overlooking Nagahama Bay. Images covered both sites (E and W) and the ferry berth in Nagahama Bay.

Images recorded on 4 August 2008 are shown in Figure 6, with turbidity cross-sections. During high tide, green-colored seawater entered the bay. During low tide, the orange-brown water flowed out from the E and W sites through both sides of the bay. The turbidity cross-section is consistent with this change in the color of surface water.

Heavy rains affected the turbidity on 9 April 2009, as shown in images taken at approximately 5 min intervals from 17.33 hours local time (Fig. 7). At approximately 17.30 hours the rains became extremely heavy. A distinct color change where orange-brown waters quickly flowed out from the beach area (Fig. 7) occurred in the study area within 10 min starting from 17.45 hours.

SEDIMENTATION OF FE-OXYHYDROXIDES

Formation of the Fe-oxyhydroxides around Satsuma Iwo-Jima Island most likely results from oxidation of Fe^{2+} in acidic low-temperature hydrothermal fluids on neutralization by mixing with seawater. The acidic low-temperature hydrothermal fluids have Fe concentrations of 649 mg/L (Shinohara *et al.* 1993) and pH 5.5 (Shikaura & Tazaki 2001). Such concentration of Fe is orders of magnitude higher than the typical concentration of Fe in seawater (parts per trillion). The turbid portions of the water column within the bay have pH 7.2–7.6, a range that is more acidic than that of seawater. The generated Fe-oxyhydroxides have patterns of sedimentation that can be estimated from the cross-sectional images of turbidity (see Figs 4,5). In this section we explore important processes for the deposition of Fe-oxyhydroxides: (i) tide-related calm conditions; (ii) wave-related suspension and re-deposition of beach sediments; and (iii) rain-related discharge sedimentation (Fig. 8).

1. During high tide in fair weather, Nagahama Bay receives cold dense seawater along its bottom from the outer ocean. It results in movement of acidic hydrothermal fluids into the overlying water column, where precipitation of fine-grained particles of Fe-oxyhydroxides occurs, imparting an orange-brown color to the water. The colored seawater flows out to the outer ocean along the sea surface during high tide. Subsequently, the receding tide drains clear seawater along the bottom. During the neap tide, reduced seawater influx increases the amount of highly turbid water, which results in precipitation of Fe-oxyhydroxides (Fig. 8).
2. We propose two cases for the development of high turbidity, likely leading to deposition of Fe-oxyhydroxides. The first case is during the low tide of spring tide conditions when water levels reached at the lowest. Seawater in the lower water column flows out of the bay, and the orange-brown hydrothermal fluids move downward (Figs 4,5). However, the tidal current was

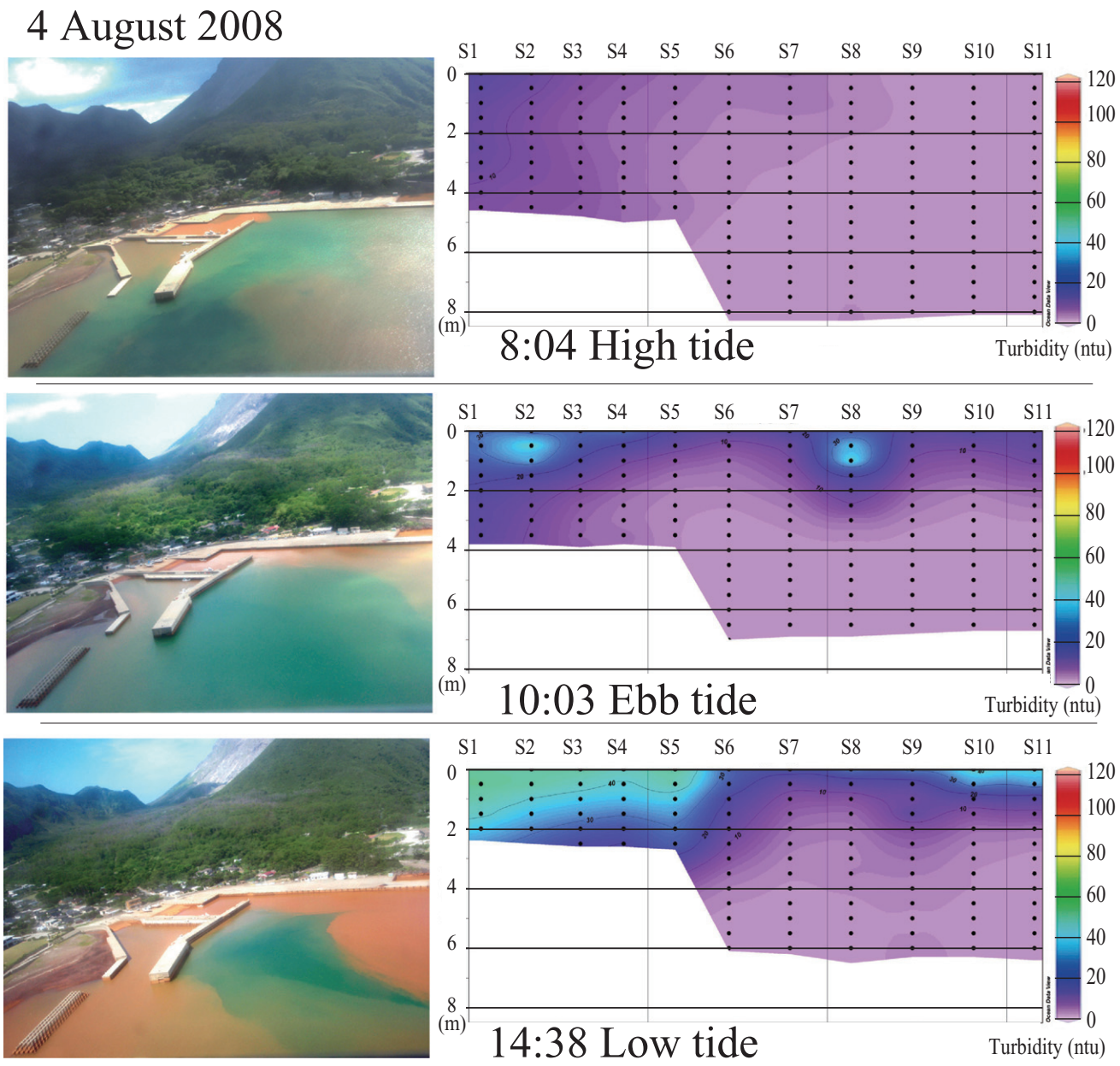

Fig. 6 Photographs of Nagahama Bay and cross-sectional images for turbidity changes during spring tide on 4 August 2008. Data on cross-sectional images are the same as those shown in Figure 5b. At high tide, clear seawater enters the bay, while at low tide, orange-brown hydrothermal fluids move out from the surface and along both sides (ferry port and west beach) of the bay.

the strongest during the spring tide, inhibiting the deposition of fine-grained materials. The second case for high turbidity is the neap tide when sluggish tidal currents limit the exchange of seawater with the outer ocean. The neap tide data in 2008 (Fig. 5) show that turbidity was higher than during spring tide due to a reduced exchange with seawater and limited outflow, which resulted in increased accumulation of Fe-oxyhydroxides.

The extent of orange-brown hydrothermal fluids in the bay was also influenced by strong waves. During periods of strong waves associated with storms, typhoons or southerly winds, the sediments in the bay with only 5–10 m water depth even during high tide are mixed and reworked to increase turbidity. The presence of sand-sized particles in sediment traps shows that sand-size fractions can be suspended by storm waves. Such suspended materials resulted in new deposition on the eroded surface.

3. Heavy rain also influences the extent of orange-brown hydrothermal fluids in the bay. During percolation of rainwater through

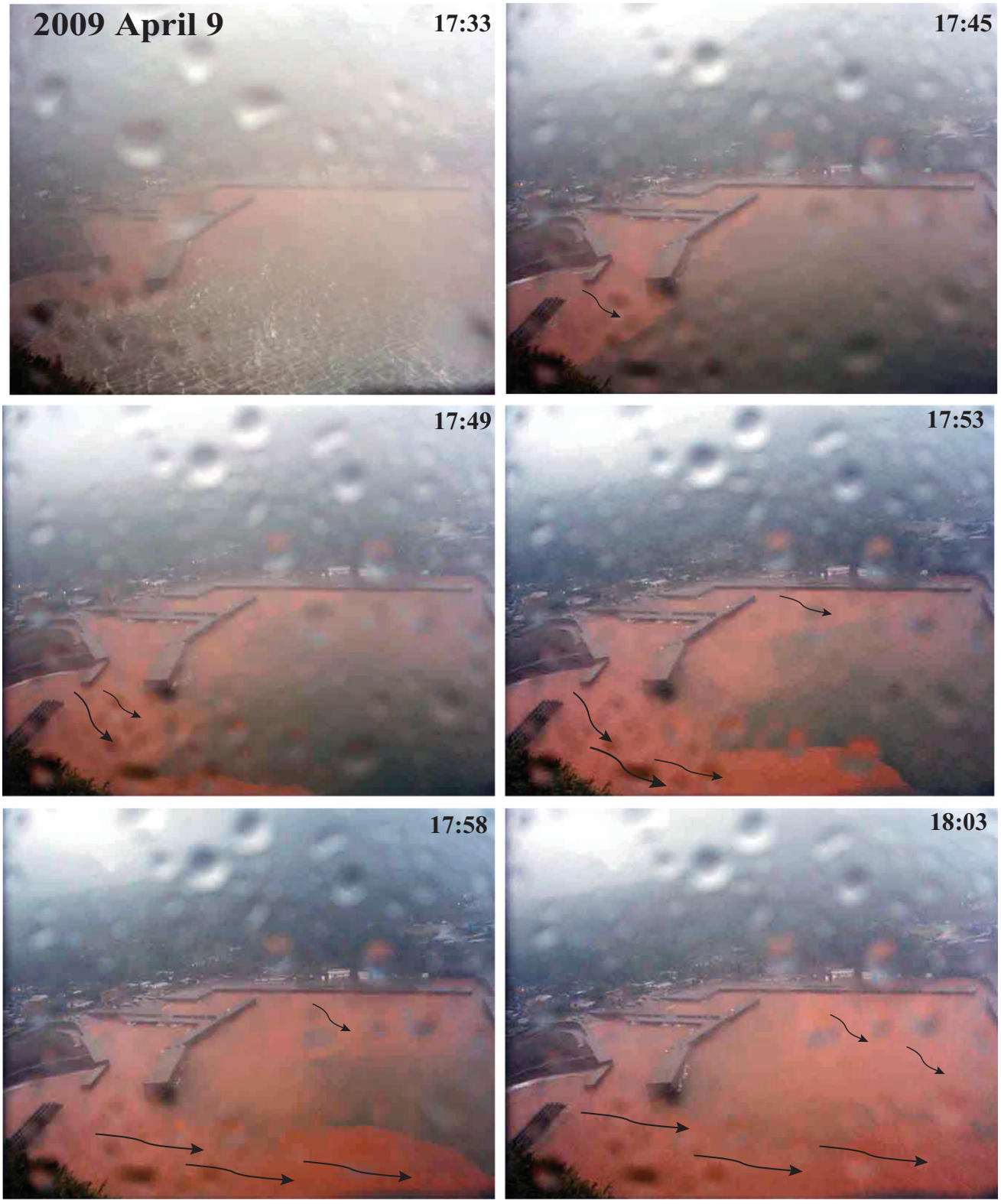

Fig. 7 Images showing the effect of rainfall on the sea surface of Nagahama Bay. Within 10 min after the start of heavy rainfall, a large volume of dark orange-colored water flowed into in the bay. Black arrows show flow directions of dark orange-colored water.

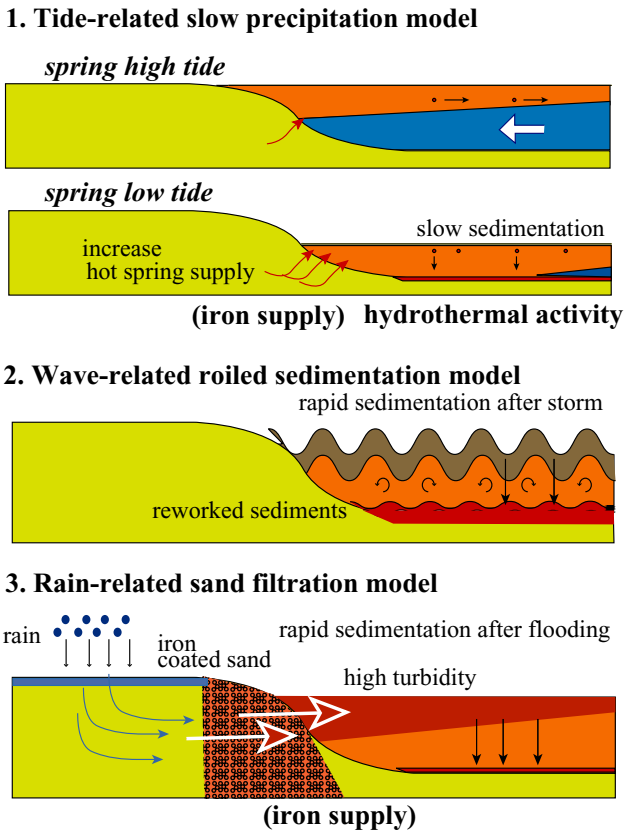

Fig. 8 Three models showing processes of Fe-oxyhydroxide sedimentation in Nagahama Bay.

Fe-oxyhydroxide-containing beach sands, Fe-oxyhydroxides would be partially removed and carried to the ocean. This process would increase turbidity and produce thick, poorly consolidated deposits in the bay.

IMPLICATIONS

Three possible sedimentary processes given in Figure 8, which may perturb pre-existing sediments, may have been recorded in ancient Fe-oxide deposits hosted in shallow-water sediments. For example, Phanerozoic ironstones may be good candidates, although their sedimentation mechanism has been poorly known (Young & Taylor 1989). They formed in shallow marine environments from roiled oolites or pellets (Robb 2005). Their source of Fe was likely Fe^{3+} colloids that were transported from fluvial environments. The deposition occurred at sea-level highstand in warm climates, where storm activity could have been vigorous, such as those during the Ordovician–Silurian and Jurassic. Effects of reworking by strong waves may be seen in a thick sequence with graded bedding features, such as that of Fe-rich sediments composed of volcaniclastic materials. This study emphasizes less explored important roles of tides and weather (storms and heavy rains) in reworking sediments in shallow marine environments, regardless of their depositional ages.

CONCLUDING REMARKS

A strong association was observed between tidal movements and water turbidity in Nagahama Bay. During high tide, clear seawater flows into the bay along the seafloor. Neutralization of acidic hydrothermal fluids with seawater promoted precipitation of Fe-oxyhydroxides. At low tide, seawater returns to the open ocean along the water surface, as does the orange-brown colored water.

With regard to the monthly cycle, the neap tide with the lowest daily amplitude marked the peak turbidity and highest concentration of Fe-oxyhydroxides. Relatively weak exchange of water with the open ocean allows precipitation of fine-grained Fe-oxyhydroxides to accumulate at the bottom.

Storm waves rework pre-existing unconsolidated Fe-oxyhydroxide-rich sediments and result in enhanced turbidity. After a storm event, the reworked sediment particles quickly settle to the bottom and may form a fining-upward sedimentary unit.

Heavy rain triggers the transport of Fe-oxyhydroxides from sands in beaches surrounding the bay. This is a newly recognized source of Fe in the study area, and may have implications for the process of iron sedimentation in larger oceanic basins. Sedimentation processes of Fe-oxyhydroxides in Nagahama Bay may improve our understanding of the formation of ancient iron-rich sedimentary sequences.

ACKNOWLEDGEMENTS

We thank the residents of the Town of Mishima, Kagoshima Prefecture for allowing us to perform fieldwork. Special thanks go to Mr. Tatsuo Ooyama, Mr. Hideyoshi Imabeppu, Mr. Hiroshi Sato, Mr. Hisataka Sato, and Mr. Goshi Hidaka for helping us during the course of our research. Professor Akihiro Kano and Dr. Susan Childers helped improve the manuscript. This research was supported by Grant-in-Aid for Scientific Research (KAKENHI) from the Ministry of Education,

Culture, Sports, Science, and Technology (MEXT) of Japan (Grant nos 18654086 and 22340151), 2006 Seed Funding Grant-in-Aid from the Japan Science and Technology Agency (JST), and Toho University Grant-in-Aid for Encouragement of Young Scientists.

REFERENCES

CONDIE K. C. 1997. *Plate Tectonics and Crustal Evolution*, 4th edn, Butterworth Heinemann, Oxford.

HEDENQUIST J. W., AOKI M. & SHINOHARA H. 1994. Flux of volatiles and ore-forming metals from the magmatic hydrothermal system of Satsuma Iwo-Jima volcano. *Geology* **22**, 585–8.

HOLLAND H. D. 1984. *The Chemical Evolution of the Atmosphere and Ocean*. Princeton University Press, Princeton, NJ.

KAGOSHIMA PREFECTURE 2008. *The Plan of the Renovation Project of Iwo-Jima Port*. Kagoshima Prefecture, Kagoshima (in Japanese).

KAMADA M. 1964. Volcanic geology and geothermal features of Satsuma Iwo-Jima, Kagoshima prefecture. *Chinetsu* **3**, 1–23 (in Japanese).

KAWANABE Y. & SAITO G. 2002. Volcanic activity of the Satsuma Iwo-Jima area during the past 6500 years. *Earth Planets and Space* **54**, 295–301.

KLEIN C. & BEUKES N. J. 1993. Sedimentology and geochemistry of the glaciogenic late Proterozoic Rapitan Iron-Formation in Canada. *Economic Geology* **88**, 542–65.

KONHAUSER K. O. & FERRIS F. G. 1996. Diversity of iron and silica precipitation by microbial mats in hydrothermal waters, Iceland: Implications for Precambrian iron formations. *Geology* **24**, 323–6.

MACHIDA H. & ARAI F. 1978. Akahoya Ash- A Holocene widespread Tephra Erupted from the Kikai Caldera, South Kyushu, Japan. *Quaternary Research* **17**, 143–63 (in Japanese with English abstract).

MAENO F. & TANIGUCHI H. 2007. Spatiotemporal evolution of a marine caldera-forming eruption, generating a low-aspect ratio pyroclastic flow, 7.3 ka, Kikai caldera, Japan: Implication from near-vent eruptive deposits. *Journal of Volcanology and Geothermal Research* **167**, 212–38.

MAENO F. & TANIGUCHI H. 2009. Sedimentation and welding processes of dilute pyroclastic density currents and fallout during a large-scale silicic eruption, Kikai caldera, Japan. *Sedimentary Geology* **220**, 227–42.

MATSUMOTO T. 1943. The four gigantic caldera volcanoes of Kyushu. *Japanese Journal of Geology and Geography* **19**, 1–57.

NINOMIYA T. & KIYOKAWA S. 2009. Time-series measurement of colored volcanic vent seawaters during a tidal cycle in Nagahama Bay, Satsuma Iwo-Jima Island, Kagoshima, Japan. *Memoirs of the Faculty of Sciences, Kyushu University, Series D, Earth and Planetary Science* **32**, 1–14.

NOGAMI K., YOSHIDA M. & OSSAKA J. 1993. Chemical composition of discolored seawater around Satsuma Iwo-Jima, Kagoshima, Japan. *Bulletin of the Volcanological Society of Japan* **38**, 71–7.

OGURI K., KITAZATO H. & GLUD R. N. 2006. Platinum octaetylporphyrin based planar optodes combined with an UV-LED excitation light source: An ideal tool for high-resolution O_2 imaging in O_2 depleted environment. *Marine Chemistry* **100**, 95–106.

OHMOTO H., WATANABE Y., YAMAGUCHI K. E. *et al.* 2006. Chemical and biological evolution of early Earth: Constraints from banded iron-formations. *In* Kesler S. E. and Ohmoto H. (eds.) *Evolution of the Early Earth's Atmosphere, Hydrosphere, and Biosphere: Constraints from Ore Deposits, Geological Society of America Memoir*, 198, pp. 291–331, Geological Society of America, Boulder, CO.

ONO K., SOYA T. & HOSONO T. 1982. *Geology of the Satsuma Iwo-Jima District*, Quadrangle Series, Scale 1:50,000. Geological Survey of Japan, Tsukuba (in Japanese with English abstract).

ROBB L. J. 2005. *Introduction to Ore-Forming Processes*. Blackwell Publishing, Oxford.

SHIBUYA T., KOMIYA T., NAKAMURA K., TAKAI K. & MARUYAMA S. 2010. Highly alkaline, high-temperature hydrothermal fluids in the early Archean ocean. *Precambrian Research* **182**, 230–8.

SHIKAURA H. & TAZAKI K. 2001. Cementations of sand grains are accelerated by microbes: Formation of bio-terrace at Satsuma Iwo-Jima Island. *Clay Science of Japan* **40**, 229–41 (in Japanese with English abstract).

SHINOHARA H., GIGGENBACH W. F., KAZAHAYA K. & HEDENQUIST J. W. 1993. Geochemistry of volcanic gases and hot springs of Satsuma-Iwojima, Japan. *Geochemical Journal* **27**, 271–85.

SHINOHARA H., KAZAHAYA K., SAITO G., MATSUSHIMA N. & KAWANABE Y. 2002. Degassing activity from Iwo-dake rhyolitic cone, Satsuma Iwo-Jima volcano, Japan: Formation of a new degassing vent, 1990–1999. *Earth Planets Space* **54**, 175–85.

SIEHL A. & THEIN J. 1989. Minette-type ironstone. *In* Young T. and Taylor W. E. G. (eds.) *Phanerozoic Ironstones*. Geological Society of London, Special Publication 46, pp. 175–93.

STANTON R. I. 1972. *Ore Petrology*. McGraw-Hill, New York.

TAKASHIMA C., OKUMURA T., NISHIDA S., KOIKE H. & KANO A. 2011. Bacterial symbiosis forming laminated iron-rich deposits in Okuoku-Hachikurou hot spring, Akita Prefecture, Japan. *Island Arc* **20**, 294–304.

TARASOV V. G., GEBRUK A. V., SHULKIN V. M. *et al.* 1999. Effect of shallow-water hydrothermal venting on the

biota of Matsupi Harbour (Rabaul Caldera, New Britain Island, Papua New Guinea). *Continental Shelf Research* **19**, 79–116.

TARASOV V. G., GEBRUK A. V., MIRONOV A. N. & MOSKALEV L. I. 2005. Deep-sea and shallow-water hydrothermal vent communities: Two different phenomena. *Chemical Geology* **224**, 5–39.

YOUNG T. P. & TAYLOR G. W. E. 1989. *Phanerozoic Ironstones*. Geological Society of London, Special Publication 46.